ARTICLES IN ENGLISH

CHEMISTRY

INORGANIC AND ANALYTICAL CHEMISTRY

Статья поступила в редакцию: 18.09.2026
Статья принята к публикации: 23.09.2026
Статья опубликована: 07.10.2026

УДК 546.302

DOI: 10.32743/UniChem.2026.148.10.23474

Coordination mode, protein targets and ADMET profile of a zinc(II) complex with phenylglyoxylic acid thiosemicarbazone

Akhatov Javokhirkhon
Doctoral student
Termez State University
Republic of Uzbekistan, Termez
E-mail: javohirxonahatov2@gmail.com

Turaev Khayit
doctor of Chemistry, Professor
Termez State University
Republic of Uzbekistan, Termez

Ashurov Jamshid
doctor of Chemistry, Professor
Institute of Bioorganic Chemistry named after Academician Obid Sodikov Academy of Sciences of the Republic of Uzbekistan
Republic of Uzbekistan, Tashkent

Библиографическое описание: Ахатов Ж.К.У., Тураев Х.Х., Ашуров Ж.М. Способ координации, белковые мишени и ADMET-профиль комплекса цинка(II) с тиосемикарбазоном фенилглиоксиловой кислоты // Universum: химия и биология : электрон. научн. журн. 2026. 10(148). URL: https://7universum.com/ru/nature/archive/item/23474

For citation: Akhatov J., Turaev K., Ashurov J. Coordination mode, protein targets and admet profile of a zinc(II) complex with phenylglyoxylic acid thiosemicarbazone // Universum: Chemistry and Biology : electronic scientific journal. 2026. No. 10(148). Available at: https://7universum.com/ru/nature/archive/item/23474

Способ координации, белковые мишени и ADMET-профиль комплекса цинка(II) с тиосемикарбазоном фенилглиоксиловой кислоты

Ахатов Жавохирхан Камол угли
докторант
Термезский государственный университет
Республика Узбекистан, г. Термез

Тураев Хайит Худайназарович
д-р хим. наук, проф.
Термезский государственный университет
Республика Узбекистан, г. Термез

Ашуров Жамшид Менгнорович
д-р хим. наук, проф.
Институт биоорганической химии имени академика Обида Содикова
Академия наук Республики Узбекистан
Республика Узбекистан, г. Ташкент

Abstract

Phenylglyoxylic acid thiosemicarbazone (H_2L) binds zinc(II) through the azomethine nitrogen, the thione sulfur and a carboxylate oxygen. This work compares the infrared spectra of ligand and complex, docks both into the ATP-binding domain of *Escherichia coli* DNA gyrase B, and computes a target and ADMET profile. Loss of ν(C=O) at 1670 cm^{-1}, carboxylate bands at 1610/1597 and 1390/1375 cm^{-1} separated by Δν = 220–222 cm^{-1}, and shifts of −27 cm^{-1} in ν(C=N) and −15 cm^{-1} in thioamide IV confirm carboxylate deprotonation and donation from N and S; the magnitude of Δν excludes symmetric bidentate chelation. In the coumarin-binding site the free ligand and a mononuclear [Zn(L)(H_2O)] fragment score alike (−6.71 and −6.75 kcal mol^{-1}) and share hydrogen bonds to Asn46 and Thr165. Two independent ligand-based methods converge on papain-family cysteine proteases — cathepsins L, K and B at 21.8, 10.4 and 8.4 % by SwissTargetPrediction, cruzipain (P_a = 0.641) and rhodesain (0.526) by PASS — the same N,S donor pair that binds the metal. Six of the seven drug-likeness descriptors lie inside their published limits; the single violation is Ghose, which follows from a WLOGP of −1.00. Mutagenicity is the only hazard on which two independently trained servers agree. No biological testing was performed; the calculations state testable hypotheses and name two experiments.

Аннотация

Тиосемикарбазон фенилглиоксиловой кислоты (H_2L) связывает цинк(II) азометиновым азотом, тионной серой и карбоксилатным кислородом. В работе сопоставлены ИК-спектры лиганда и комплекса, проведён докинг в АТФ-связывающий домен ДНК-гиразы B *Escherichia coli*, рассчитаны вероятные белковые мишени и ADMET-профиль. Исчезновение ν(C=O) при 1670 $см^{-1}$, появление полос карбоксилат-иона при 1610/1597 и 1390/1375 $см^{-1}$ с Δν = 220–222 $см^{-1}$ и смещения ν(C=N) на −27 $см^{-1}$ и тиоамидной полосы IV на −15 $см^{-1}$ подтверждают депротонирование карбоксильной группы и участие N и S в координации; величина Δν исключает симметричную бидентатную хелатацию. В центре связывания кумаринов свободный лиганд и моноядерный фрагмент [Zn(L)(H_2O)] получают близкие оценки (−6,71 и −6,75 ккал/моль) и общие водородные связи с Asn46 и Thr165. Два независимых лиганд-

ориентированных метода указывают на цистеиновые протеазы папаинового семейства: катепсины L, K и B (21,8; 10,4 и 8,4 %) по SwissTargetPrediction, круципаин (P_a = 0,641) и родезаин (0,526) по PASS — то есть на тот же донорный набор N,S, который связывает металл. Шесть из семи дескрипторов лекарственного подобия лежат в опубликованных границах; единственное нарушение — правило Ghose, следующее из WLOGP = −1,00. Два независимо обученных сервера сходятся лишь на одном риске — мутагенности. Биологические испытания не проводились; расчёты формулируют проверяемые гипотезы и указывают два конкретных эксперимента.

Keywords: thiosemicarbazone, zinc(II) complex, infrared spectroscopy, carboxylate coordination mode, molecular docking, DNA gyrase B, target prediction, cysteine proteases, ADMET.

Ключевые слова: тиосемикарбазон, комплекс цинка(II), ИК-спектроскопия, способ координации карбоксилат-иона, молекулярный докинг, ДНК-гираза B, предсказание мишеней, цистеиновые протеазы, ADMET.

Introduction

Thiosemicarbazones remain useful ligands because the N–N–C(=S) fragment places a hard nitrogen donor and a soft sulfur donor on adjacent atoms, and because deprotonation of the hydrazinic nitrogen converts a neutral chelator into an anionic one without altering the donor set [22, 5]. Attaching a carboxylic acid to the carbon that bears the azomethine nitrogen, as in the thiosemicarbazones of α-keto acids, adds two oxygen donors: three of the four saturate one metal while the fourth reaches a neighbouring one.

In the zinc(II) complex of phenylglyoxylic acid thiosemicarbazone the doubly deprotonated ligand chelates one metal through the azomethine nitrogen, the thione sulfur and one carboxylate oxygen, and donates its second carboxylate oxygen to a symmetry-related metal, giving a five-coordinate $ZnNO_3S$ chromophore (single-crystal X-ray diffraction; see Materials and methods). Thiosemicarbazones of α-keto acids are much less studied than those of aldehydes and ketones, and for this compound the binding mode has not been followed beyond the crystal structure.

Whether that mode is visible outside a diffraction experiment is the first question taken up here: the separation of the two carboxylate stretching modes depends on whether the group chelates one metal or bridges two, so the infrared spectrum should report on the binding mode directly. The second is whether the molecular unit from which the coordination sphere is built can occupy a defined protein site. The third, answerable only by methods that search chemical space rather than a single pocket, is which protein families the scaffold resembles and whether the resulting profile is worth developing. Vibrational assignment, docking, ligand-based target prediction and computed developability follow in that order. No antibacterial or cytotoxicity measurements are reported, so every computational result below is a hypothesis, and the applicability limits of each method are stated where they matter.

Materials and methods

Infrared spectroscopy

Infrared spectra of the free ligand and of the complex were measured under identical conditions on one WQF-530A instrument (Beijing Beifen-Ruili Analytical Instrument (Group) Co., Ltd., Beijing, China) over 4000–400 cm^{-1} at a resolution of 4 cm^{-1}, using a Specac Quest single-reflection attenuated total reflectance (ATR) accessory with a diamond crystal puck (Specac Ltd, Orpington, UK). Band positions were taken from the data rather than read off the plot: the transmittance trace was inverted and its local minima located with the find_peaks routine of SciPy 1.18.1 [32] at a prominence threshold of 0.4 % transmittance, which returned 24 bands for H_2L and 76 for the complex above 450 cm^{-1}. The sharp doublet at 2360/2341 cm^{-1} in the complex spectrum is atmospheric CO_2 rather than a sample band; signal below roughly 420 cm^{-1} approaches the cut-off of the optical arrangement and was left uninterpreted.

Ligand models, receptor and docking

Two discrete models were built from the refined atomic coordinates of the single-crystal X-ray structure of this compound. The first is the metal-free ligand in its neutral form, connectivity taken from the refined geometry, SMILES NC(=S)NN=C(C(=O)O)c1ccccc1, matching PubChem CID 71951536 [19]; its three-dimensional structure was generated with the ETKDG algorithm [29] and minimized with the MMFF94 force field [17] in RDKit 2026.03.6 [28]. The second is the mononuclear fragment [Zn(L)(H_2O)], obtained by cutting the bridging Zn–O contact and retaining the symmetry-generated metal with its aqua ligand. Nothing was optimized and no atoms were added, so the coordination distances of the refined structure are reproduced to better than 0.001 Å. The site vacated by the cut is the one the bridge occupies in the solid, and is treated as the position available to a protein donor atom.

The receptor was the 24 kDa ATPase domain of *E. coli* DNA gyrase B, a validated antibacterial target [6], in complex with clorobiocin (PDB entry 1KZN [20]). Chain A was retained (186 residues, 1446 non-hydrogen atoms); waters, the co-crystallized inhibitor and alternative conformations were removed with GEMMI 0.7.5 [35] and hydrogen atoms added at pH 7.4 with Open Babel 3.2.1 [26]. Docking used AutoDock Vina 1.2.5 [30, 11] with the Vina scoring function, a 22 × 25 × 25 Å box centred on the clorobiocin centroid (19.150, 30.393, 34.745), exhaustiveness 32, nine retained modes, seed 42 and four CPU threads. The ligand file was prepared with Meeko 0.8.0 and retained four torsional degrees of freedom; the metal fragment was docked as a rigid body with zinc mapped to the metal-donor type of the Vina force field. Contacts of the best pose were profiled with PLIP 3.0.1 [1].

Prediction servers and the structure submitted to them

Targets were predicted with SwissTargetPrediction [7] and SwissSimilarity [36] against DrugBank [34] and with PASS Online [13]; descriptors and drug-likeness came from SwissADME [8], pharmacokinetic and toxicological endpoints from pkCSM [27] and ProTox-3.0 [3].

SwissADME's own export records the submitted structure as [O-]C(=O)C(=NN=C(N)[S-])c1ccccc1.[Zn^{+2}] — the doubly deprotonated ligand and the zinc dication written as separate ionic species, formula $C_9H_7N_3O_2SZn$, M_r = 286.62; the pkCSM depiction shows the same disconnected arrangement. This sets an applicability limit on every server result below. These services are trained on organic, drug-like molecules and none parameterizes a coordinated transition metal. With a zinc salt entered as disconnected ions the descriptors are therefore essentially those of the organic dianion, the metal contributing to formula and mass but to no electronic or steric term. For comparison, descriptors of the neutral free ligand were computed locally with RDKit [28] together with the PAINS [2] and Brenk [4] substructure filters, and log *D* at pH 7.4 and the most acidic pK_a were predicted with the public log *D* and pK_a models of an external machine-learning service (Inductive Bio), each prediction carrying an in-domain flag.

Results and discussion

Infrared spectra: donor atoms and the carboxylate mode

Four independent changes between the two spectra identify the coordinating atoms (Figure 1, Table 1).

The strong ν(C=O) band of the carboxylic acid at 1670 cm^{-1} has no counterpart in the complex; in its place two strong bands appear at 1610 and 1597 cm^{-1} and a second pair at 1390 and 1375 cm^{-1}, the pattern expected for a carboxylate formed by deprotonation and coordination [9, 25].

The separation of these modes carries geometric information. For corresponding members of each pair, $\Delta\nu = \nu_{as} - \nu_s$ = 220–222 cm^{-1}, a value that belongs to a carboxylate whose two oxygen atoms are inequivalent and that excludes the symmetric bidentate chelation at a single metal which compresses it [9]. A bridging carboxylate produces exactly this, each metal seeing an essentially unidentate donor. Because the spectrum of the corresponding ionic salt was not measured, the Deacon–Phillips criterion is applied here qualitatively, as a consistency test rather than an independent structure determination.

The azomethine stretch moves from 1585 to 1558 cm^{-1}. A shift of −27 cm^{-1} is what coordination of the imine nitrogen produces, donation of the nitrogen lone pair weakening the C=N bond [22, 25]. The thioamide IV band, largely ν(C=S), shifts from 850 to 835 cm^{-1} and the thioamide III region from 1124/1074 to 1072/1036 cm^{-1}, both consistent with sulfur donation.

Two further changes confirm the composition: the ligand's three N–H bands collapse to a single feature at 3138 cm^{-1} once the hydrazinic proton is lost, and a broad band at 3442 cm^{-1} appears from coordinated and lattice water. Four weak bands at 503–472 cm^{-1} lie where ν(Zn–N) and ν(Zn–O) are expected and are assigned only tentatively; ν(Zn–S), expected near 300–350 cm^{-1}, falls outside the measured range, so the zinc–sulfur bond cannot be confirmed by a direct band.

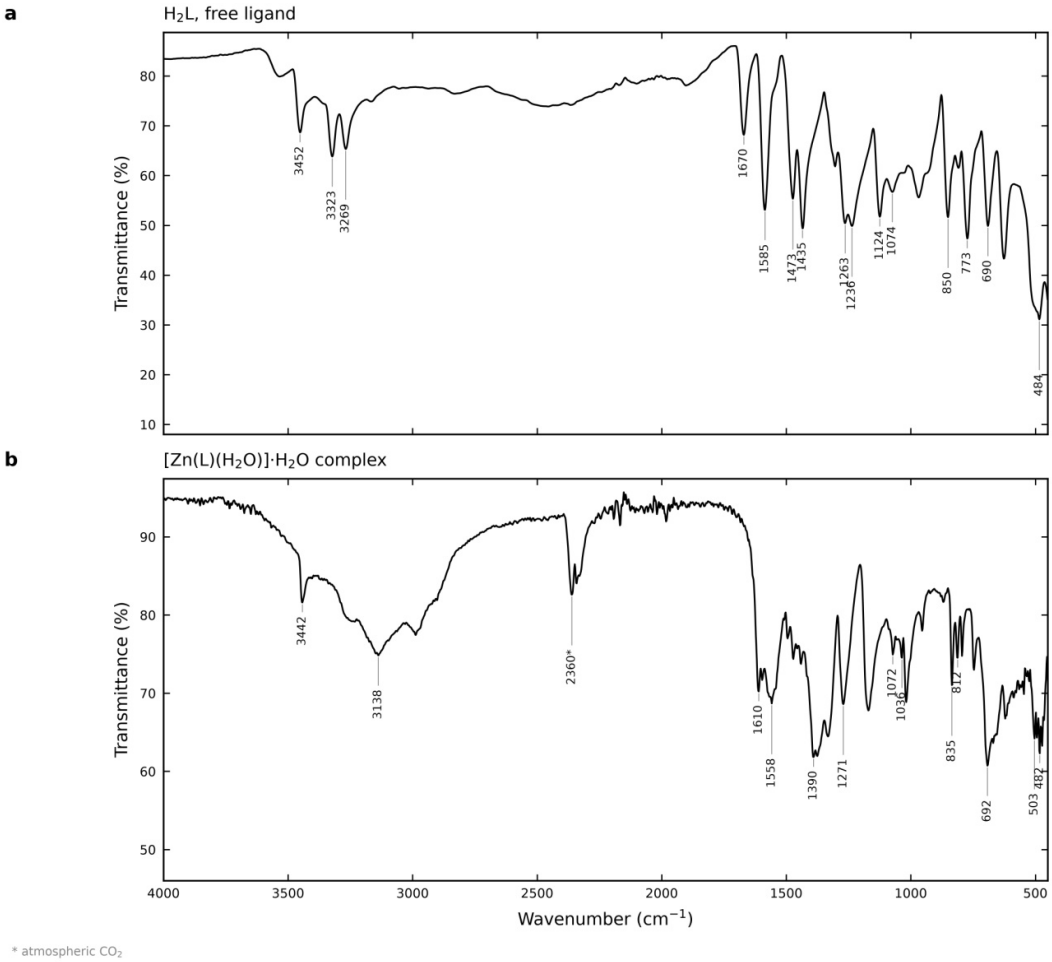


Figure 1. Infrared spectra of (a) the free ligand H_2L and (b) the zinc(II) complex. Band positions are printed as vertical labels; the asterisk marks atmospheric CO_2

Table 1.

Infrared band assignments for the free ligand H2L and the zinc(II) complex. Positions in cm⁻¹

Assignment	H_2L / cm⁻¹	Complex / cm⁻¹	Comment
ν(O–H), lattice + coordinated water	3533 (w)	3442 (br, s)	broad band appears on complexation — aqua ligand and lattice water
ν(N–H), NH_2 asym/sym + hydrazinic N–H	3452, 3323, 3269	3138	three N–H bands collapse to one; hydrazinic N2–H lost on deprotonation
ν(C=O), COOH	1670 (s)	absent	carboxylic acid consumed by deprotonation and coordination
$\nu_{as}(COO^-)$	absent	1610, 1597 (s)	new asymmetric carboxylate stretch
ν(C=N), azomethine	1585 (vs)	1558 (s)	−27 cm⁻¹ shift; N1 coordination
δ(NH_2) / ring modes	1473, 1435	1495, 1471, 1441	skeletal
$\nu_s(COO^-)$	absent	1390, 1375 (s)	Δν = 220–222 cm⁻¹
thioamide II, ν(C=N) + ν(C–N)	1263, 1236	1271	band pair merges
thioamide III, ν(C–N) + ν(C=S)	1124, 1074	1072, 1036	shift to lower wavenumber
thioamide IV, ν(C=S)	850	835	−15 cm⁻¹ shift; S1 coordination
out-of-plane phenyl C–H	773, 690	795, 746, 692	monosubstituted phenyl retained

Assignment	H_2L / cm^{-1}	Complex / cm^{-1}	Comment
ν(Zn–N) / ν(Zn–O) region	absent	503, 494, 482, 472	tentative; ν(Zn–S) (300–350 cm^{-1}) lies below the measured range

Docking into the gyrase B coumarin site

Both models place their best pose inside the clorobiocin site, scoring −6.71 kcal mol^{-1} for H_2L and −6.75 kcal mol^{-1} for the mononuclear fragment, and their nine retained poses span the same narrow range (Figure 2a).

These numbers are not a ranking. The Vina function is parameterized for organic ligands and carries no metal-specific term, so the fragment value is an empirical estimate rather than a metal-aware interaction energy, and the difference of 0.04 kcal mol^{-1} lies far inside the method's scoring error of about 2 kcal mol^{-1}. Only the qualitative statement is defensible: both species are accommodated with comparable, moderate affinity.

The contact patterns differ in an interpretable way (Figure 2b, c). PLIP finds four hydrogen bonds for each model. The free ligand binds Asn46, Asp73 and Thr165 at 2.25, 2.42 and 2.44 Å and Val71 at 2.74 Å within a hydrophobic wall; the metal fragment keeps Asn46 and Thr165, adds Asp49 and Gly77, and directs its open coordination site at the carboxylate of Glu50 with a Zn···O distance of 3.09 Å. That distance exceeds a zinc–carboxylate bond and falls outside the 3.0 Å cut-off PLIP applies to metal coordination, so it is a near-coordination contact rather than a coordinate bond. It is nevertheless the geometric consequence of the bridging mode established above: the site that the bridging carboxylate occupies in the solid is, in the docked fragment, aimed at a protein carboxylate.

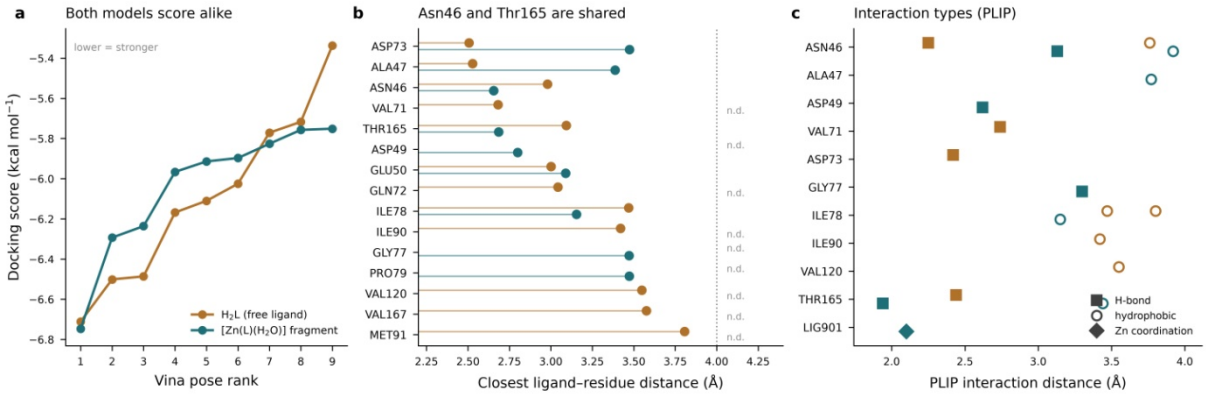


Figure 2. Docking against the ATPase domain of E. coli DNA gyrase B (PDB 1KZN, chain A). (a) Scores of the nine retained poses for each model. (b) Closest ligand–residue distance for every residue within 4 Å of the best pose; n.d. marks a residue contacted by only one model. (c) Interaction types identified by PLIP; the Zn coordination entry at 2.10 Å is internal to the ligand, not a protein contact

Ligand-based target prediction

Docking answers only about the target it is given, so the scaffold was also submitted to two methods that search chemical space (Figure 3).

SwissTargetPrediction returns 100 ranked human targets. Monoamine oxidase A (27.4 %) and the methyltransferase subunit METTL3 (27.2 %) head the list as isolated entries, but the coherent block is the next one: cathepsins L, K and B at 21.8, 10.4 and 8.4 %, three papain-family cysteine proteases, followed by further proteases down to prothrombin at 4.3 % (Figure 3a). Eight of the top twelve targets are proteases.

PASS Online, which uses a different descriptor system and a different training set, returns 395 predicted activities, one above $P_a = 0.7$ and eleven between 0.5 and 0.7 (Figure 3b). The two informative entries are cruzipain inhibitor ($P_a = 0.641$, $P_i = 0.001$) and rhodesain inhibitor (0.526, 0.001), the principal cysteine proteases of *Trypanosoma cruzi* and *T. brucei* and papain-family enzymes like the cathepsins; falcipain and falcipain 2 of *Plasmodium falciparum* follow at 0.454. The highest single prediction, HMGCS2 expression enhancer at 0.725, stands alone with no support from any other method used here.

Two methods with independent training sets and independent descriptors therefore point at the same enzyme family, and the convergence has a structural rationale: the thioamide sulfur and azomethine nitrogen that bind zinc, the donor pair identified independently by the infrared shifts above, are the pair through which thiosemicarbazones engage the catalytic cysteine environment of papain-family proteases [10, 16]. The prediction follows from the established donor set rather than being independent of it, and it names one inexpensive experiment.

Similarity screening against DrugBank gave 77 hits, only three reaching 0.5 (Figure 3c); the closest, amido phenyl pyruvic acid (DB02018) at 0.799, is another α-keto-acid derivative. The scaffold has no analogue in the purchasable subset of ZINC [18] within a Tanimoto distance of 6 and no measured affinity in BindingDB [15] above 60 % similarity, so it is a sparsely represented chemotype, which is an argument for measuring activity rather than inferring it.

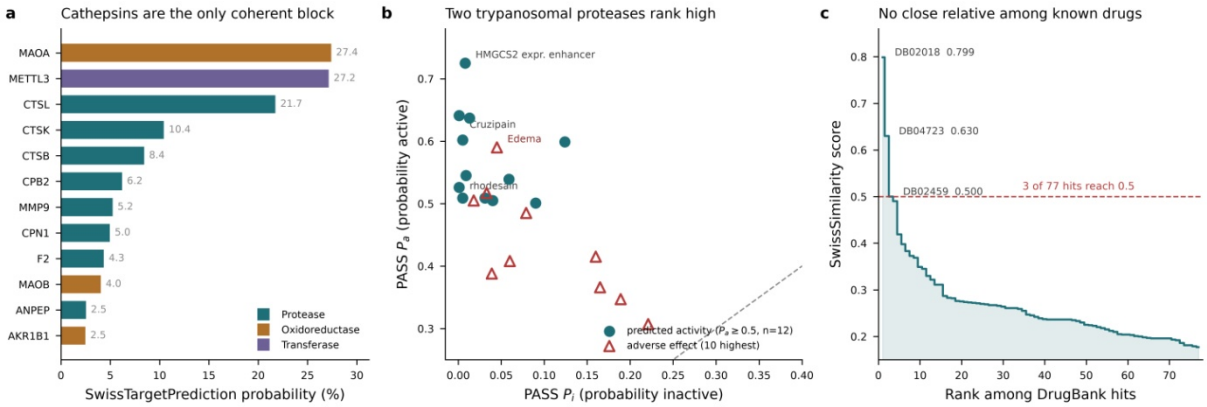


Figure 3. Ligand-based target prediction (a) The twelve highest-ranked SwissTargetPrediction targets (MAOA, METTL3, CTSL, CTSK, CTSB, CPB2, MMP9, CPN1, F2, MAOB, ANPEP, AKR1B1), coloured by target class; probabilities are printed as returned, rounded to 0.1 %. (b) The PASS activity spectrum: every predicted activity with $P_a \geq 0.5$ and the ten highest-ranked adverse effects; points far from the diagonal are the more reliable predictions. (c) SwissSimilarity scores of all 77 DrugBank hits in rank order; the three above 0.5 are amido phenyl pyruvic acid (DB02018), 2-(3-guanidinophenyl)-3-mercaptopropanoic acid (DB04723) and 4-guanidinobenzoic acid (DB02459)

Drug-likeness, ADMET and predicted hazards

Of the seven descriptors constrained by the Lipinski, Ghose, Veber and Egan filters, six fall inside their published ranges for the submitted zinc salt and for the neutral free ligand alike (Figure 4a) [12, 14, 21, 24, 31]. The exception is lipophilicity as the Ghose filter measures it: the Wildman–Crippen WLOGP of the salt is −1.00 [33], below that filter's lower bound of −0.4, and SwissADME accordingly reports one Ghose violation, the only rule violation returned for either species. The value is as much a property of the descriptor as of the compound, since the same server's consensus log *P*, averaging five models, is 0.92 and well inside the range, and the free ligand's WLOGP of 0.31 raises no violation at all.

Lipinski, Veber, Egan, Muegge and lead-likeness are satisfied without exception, with a bioavailability score of 0.55. No PAINS alert is raised, and the three Brenk alerts returned — the imine, the thiocarbonyl and the N–N single bond — belong to the thiosemicarbazone pharmacophore itself and cannot be removed without removing the donor set that makes the ligand coordinate. A predicted most acidic pK_a of 3.52 places the carboxylic acid essentially fully ionized at physiological pH, consistent with the carboxylate coordination identified spectroscopically, and a predicted log *D* of −0.92 confirms low lipophilicity for that ionized form.

Of the 45 endpoints ProTox-3.0 evaluates, seven are returned Active, five of them within 0.08 of the 0.5 decision boundary; the Inactive calls for nephrotoxicity and cardiotoxicity are equally marginal, so the organ-level predictions are too close to the threshold to guide an experiment (Figure 4b). The rest of the panel is uniformly negative, including all seven Tox21 nuclear-receptor pathways, all five stress-response pathways, all fourteen molecular initiating events and all six cytochrome P450 isoforms.

Reading the servers against one another is more informative than any of them alone (Figure 4c). They agree that absorption is high — gastrointestinal absorption classified as high by SwissADME, human intestinal absorption 77.8 % by pkCSM — and that the compound is no P-glycoprotein substrate. They disagree on four endpoints: CYP1A2 inhibition, where SwissADME is the outlier against two servers finding none; blood–brain penetration, where no two agree and the three values are not even on a common scale; carcinogenicity, flagged by PASS at P_a = 0.505 and Inactive by ProTox-3.0; and hepatotoxicity, better read as an absence of signal than a contradiction, its Active call sitting 0.08 above the boundary. None can be resolved computationally: each marks an endpoint where one measurement is worth more than a third prediction.

One hazard survives the comparison. pkCSM returns AMES toxicity as Yes and ProTox-3.0 returns mutagenicity as Active — two independently trained models flagging the same liability, which is a stronger statement than any single probability in this study and chemically plausible for an N–N-containing thioamide. Other pkCSM toxicity endpoints are unremarkable: no hERG inhibition, no skin sensitisation, a maximum tolerated dose of 0.337 log mg kg^{-1} day^{-1}.

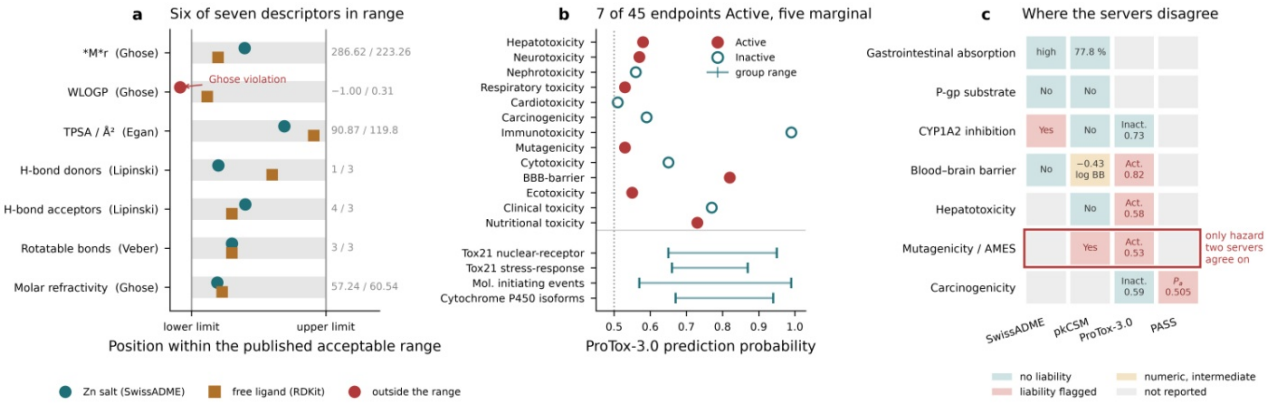


Figure 4. Computed developability profile (a) Each descriptor plotted as its position within the published acceptable range of the rule that constrains it, for the submitted zinc salt and for the neutral free ligand; the grey band is the compliant interval and the numbers at the right are the actual values (salt / ligand). The lipophilicity row is WLOGP, the descriptor the Ghose filter tests, and the salt lies below its lower bound — the single rule violation of the whole panel; the consensus log P of the same species, 0.92, is inside the range. (b) All 45 ProTox-3.0 endpoints: the 13 organ-toxicity and general endpoints individually, filled symbols marking Active calls, and the four uniformly Inactive groups shown as probability ranges (Tox21 nuclear-receptor 0.65–0.95, Tox21 stress-response 0.66–0.87, molecular initiating events 0.57–0.99, cytochrome P450 0.67–0.94). (c) Endpoints predicted by more than one server, coloured by whether that server reports a liability; the boxed row is the only hazard on which two servers agree

Conclusion

The four analyses answer to one another. Comparative infrared spectroscopy fixes the coordination mode at four independent points, the most diagnostic being the carboxylate separation of 220–222 cm^{-1}, which excludes symmetric chelation and leaves a bridging carboxylate. That mode fixes the shape of the molecular unit used for docking: with one carboxylate oxygen committed to a neighbouring metal, the fragment cut from that environment necessarily carries a free coordination

site, and it is this site that faces Glu50 in the docked pose. Both the free ligand and that fragment are accommodated in the coumarin-binding site of the *E. coli* gyrase B ATPase domain with comparable scores and a shared Asn46/Thr165 anchor. Independently of that calculation, SwissTargetPrediction and PASS Online converge on papain-family cysteine proteases, recognizing the same N,S donor pair that the infrared shifts identify, so the assignment carries structural meaning rather than statistical coincidence. The computed profile is permissive rather than encouraging: absorption is high and six of seven drug-likeness descriptors are in range, but nothing singles the compound out.

Three limitations bound these results. Every server prediction comes from models trained on organic drug-like molecules, while the submitted structure is a zinc salt written as disconnected ions, outside those models' applicability domain. The mononuclear fragment is a model of a coordination environment and has not been shown to exist as a discrete species in solution. And no antibacterial, enzymatic or cytotoxicity measurement is reported, so no claim is made that the complex or the ligand inhibits DNA gyrase, a cathepsin or any other target. The same three points name the experiments that would settle them: a cathepsin L or B inhibition assay, a bacterial reverse-mutation assay [23], and a solution-speciation measurement to establish what the compound is under assay conditions.

References

1. Adasme M.F., Linnemann K.L., Bolz S.N., Kaiser F., Salentin S., Haupt V.J., Schroeder M. PLIP 2021: expanding the scope of the protein–ligand interaction profiler to DNA and RNA // Nucleic Acids Research. – 2021. – Vol. 49. – DOI: 10.1093/nar/gkab294.
2. Baell J.B., Holloway G.A. New substructure filters for removal of pan assay interference compounds (PAINS) from screening libraries and for their exclusion in bioassays // Journal of Medicinal Chemistry. – 2010. – Vol. 53. – P. 2719–2740. – DOI: 10.1021/jm901137j.
3. Banerjee P., Kemmler E., Dunkel M., Preissner R. ProTox 3.0: a webserver for the prediction of toxicity of chemicals // Nucleic Acids Research. – 2024. – Vol. 52. – DOI: 10.1093/nar/gkae303.
4. Brenk R., Schipani A., James D., Krasowski A., Gilbert I.H., Frearson J., Wyatt P.G. Lessons learnt from assembling screening libraries for drug discovery for neglected diseases // ChemMedChem. – 2008. – Vol. 3. – P. 435–444. – DOI: 10.1002/cmdc.200700139.
5. Casas J., García-Tasende M., Sordo J. Main group metal complexes of semicarbazones and thiosemicarbazones. A structural review // Coordination Chemistry Reviews. – 2000. – Vol. 209. – P. 197–261. – DOI: 10.1016/S0010-8545(00)00363-5.
6. Collin F., Karkare S., Maxwell A. Exploiting bacterial DNA gyrase as a drug target: current state and perspectives // Applied Microbiology and Biotechnology. – 2011. – Vol. 92. – P. 479–497. – DOI: 10.1007/s00253-011-3557-z.
7. Daina A., Michielin O., Zoete V. SwissTargetPrediction: updated data and new features for efficient prediction of protein targets of small molecules // Nucleic Acids Research. – 2019. – Vol. 47. – DOI: 10.1093/nar/gkz382.

8. Daina A., Michielin O., Zoete V. SwissADME: a free web tool to evaluate pharmacokinetics, drug-likeness and medicinal chemistry friendliness of small molecules // Scientific Reports. – 2017. – Vol. 7. – DOI: 10.1038/srep42717.
9. Deacon G.B., Phillips R.J. Relationships between the carbon-oxygen stretching frequencies of carboxylato complexes and the type of carboxylate coordination // Coordination Chemistry Reviews. – 1980. – Vol. 33. – P. 227–250. – DOI: 10.1016/S0010-8545(00)80455-5.
10. Du X., Guo C., Hansell E., Doyle P.S., Caffrey C.R., Holler T.P. McKerrow J.H., Cohen F.E. Synthesis and structure–activity relationship study of potent trypanocidal thiosemicarbazone inhibitors of the trypanosomal cysteine protease cruzain // Journal of Medicinal Chemistry. – 2002. – Vol. 45. – P. 2695–2707. – DOI: 10.1021/jm010459j.
11. Eberhardt J., Santos-Martins D., Tillack A.F., Forli S. AutoDock Vina 1.2.0: new docking methods, expanded force field, and Python bindings // Journal of Chemical Information and Modeling. – 2021. – Vol. 61. – P. 3891–3898. – DOI: 10.1021/acs.jcim.1c00203.
12. Egan W.J., Merz K.M. Jr., Baldwin J.J. Prediction of drug absorption using multivariate statistics // Journal of Medicinal Chemistry. – 2000. – Vol. 43. – P. 3867–3877. – DOI: 10.1021/jm000292e.
13. Filimonov D.A., Lagunin A.A., Gloriozova T.A., Rudik A.V., Druzhilovskii D.S., Pogodin P.V., Poroikov V.V. Prediction of the biological activity spectra of organic compounds using the PASS Online web resource // Chemistry of Heterocyclic Compounds. – 2014. – Vol. 50. – P. 444–457. – DOI: 10.1007/s10593-014-1496-1.
14. Ghose A.K., Viswanadhan V.N., Wendoloski J.J. A knowledge-based approach in designing combinatorial or medicinal chemistry libraries for drug discovery. 1. A qualitative and quantitative characterization of known drug databases // Journal of Combinatorial Chemistry. – 1998. – Vol. 1. – P. 55–68. – DOI: 10.1021/cc9800071.
15. Gilson M.K., Liu T., Baitaluk M., Nicola G., Hwang L., Chong J. BindingDB in 2015: a public database for medicinal chemistry, computational chemistry and systems pharmacology // Nucleic Acids Research. – 2015. – Vol. 44. – DOI: 10.1093/nar/gkv1072.
16. Greenbaum D.C., Mackey Z., Hansell E., Doyle P., Gut J., Caffrey C.R., Lehrman J., Rosenthal P.J. McKerrow J.H., Chibale K. Synthesis and structure–activity relationships of parasiticidal thiosemicarbazone cysteine protease inhibitors against Plasmodium falciparum, Trypanosoma brucei, and Trypanosoma cruzi // Journal of Medicinal Chemistry. – 2004. – Vol. 47. – P. 3212–3219. – DOI: 10.1021/jm030549j.
17. Halgren T.A. Merck molecular force field. I. Basis, form, scope, parameterization, and performance of MMFF94 // Journal of Computational Chemistry. – 1996. – Vol. 17. – P. 490–519. – DOI: 10.1002/(SICI)1096-987X(199604)17:5/6<490::AID-JCC1>3.0.CO;2-P.
18. Irwin J.J., Tang K.G., Young J., Dandarchuluun C., Wong B.R., Khurelbaatar M., Moroz Y.S., Mayfield J., Sayle R.A. ZINC20 – a free ultralarge-scale chemical database for ligand discovery // Journal of Chemical Information and Modeling. – 2020. – Vol. 60. – P. 6065–6073. – DOI: 10.1021/acs.jcim.0c00675.

19. Kim S., Chen J., Cheng T., Gindulyte A., He J., He S., Li Q., Shoemaker B.A., Thiessen P.A., Yu B. PubChem 2023 update // Nucleic Acids Research. – 2023. – Vol. 51. – DOI: 10.1093/nar/gkac956.
20. Lafitte D., Lamour V., Tsvetkov P.O., Makarov A.A., Klich M., Deprez P., Moras D., Bri, C., Gilli R. DNA gyrase interaction with coumarin-based inhibitors: the role of the hydroxybenzoate isopentenyl moiety and the 5′-methyl group of the noviose // Biochemistry. – 2002. – Vol. 41. – P. 7217–7223. – DOI: 10.1021/bi0159837.
21. Lipinski C.A., Lombardo F., Dominy B.W., Feeney P.J. Experimental and computational approaches to estimate solubility and permeability in drug discovery and development settings // Advanced Drug Delivery Reviews. – 1997. – Vol. 23. – P. 3–25. – DOI: 10.1016/S0169-409X(96)00423-1.
22. Lobana T.S., Sharma R., Bawa G., Khanna S. Bonding and structure trends of thiosemicarbazone derivatives of metals – An overview // Coordination Chemistry Reviews. – 2009. – Vol. 253. – P. 977–1055. – DOI: 10.1016/j.ccr.2008.07.004.
23. Mortelmans K., Zeiger E. The Ames Salmonella/microsome mutagenicity assay // Mutation Research – Fundamental and Molecular Mechanisms of Mutagenesis. – 2000. – Vol. 455. – P. 29–60. – DOI: 10.1016/S0027-5107(00)00064-6.
24. Muegge I., Heald S.L., Brittelli D. Simple selection criteria for drug-like chemical matter // Journal of Medicinal Chemistry. – 2001. – Vol. 44. – P. 1841–1846. – DOI: 10.1021/jm015507e.
25. Nakamoto K. Infrared and Raman spectra of inorganic and coordination compounds. Part B: Applications in coordination, organometallic, and bioinorganic chemistry. – 6-th ed. – Hoboken: John Wiley & Sons, 2009.
26. O’Boyle N.M., Banck M., James C.A., Morley C., Vandermeersch T., Hutchison G.R. Open Babel: an open chemical toolbox // Journal of Cheminformatics. – 2011. – Vol. 3. – DOI: 10.1186/1758-2946-3-33.
27. Pires D.E.V., Blundell T.L., Ascher D.B. pkCSM: predicting small-molecule pharmacokinetic and toxicity properties using graph-based signatures // Journal of Medicinal Chemistry. – 2015. – Vol. 58. – P. 4066–4072. – DOI: 10.1021/acs.jmedchem.5b00104.
28. RDKit: Open-source cheminformatics. Version 2026.03.6. – Retrived from: (accessed date: 17.09.2026) – URL: https://www.rdkit.org. (accessed 07.10.2026)
29. Riniker S., Landrum G.A. Better informed distance geometry: using what we know to improve conformation generation // Journal of Chemical Information and Modeling. – 2015. – Vol. 55. – P. 2562–2574. – DOI: 10.1021/acs.jcim.5b00654.
30. Trott O., Olson A.J. AutoDock Vina: improving the speed and accuracy of docking with a new scoring function, efficient optimization, and multithreading // Journal of Computational Chemistry. – 2010. – Vol. 31. – P. 455–461. – DOI: 10.1002/jcc.21334.
31. Veber D.F., Johnson S.R., Cheng H., Smith B.R., Ward K.W., Kopple K.D. Molecular properties that influence the oral bioavailability of drug candidates // Journal of Medicinal Chemistry. – 2002. – Vol. 45. – P. 2615–2623. – DOI: 10.1021/jm020017n.

32. Virtanen P., Gommers R., Oliphant T.E., Haberl, M., Reddy T., Cournapeau D., Burovski E., Peterson P., Weckesser W., Bright J. SciPy 1.0: fundamental algorithms for scientific computing in Python // Nature Methods. – 2020. – Vol. 17. – P. 261–272. – DOI: 10.1038/s41592-019-0686-2.
33. Wildman S.A., Crippen G.M. Prediction of physicochemical parameters by atomic contributions // Journal of Chemical Information and Computer Sciences. – 1999. – Vol. 39. – P. 868–873. – DOI: 10.1021/ci990307l.
34. Wishart D.S., Feunang Y.D., Guo A.C., Lo E.J., Marcu A., Grant J.R., Sajed T., Johnson D., Li C., Sayeeda Z. DrugBank 5.0: a major update to the DrugBank database for // Nucleic Acids Research. – 2018. – Vol. 46. – DOI: 10.1093/nar/gkx1037.
35. Wojdyr M. GEMMI: a library for structural biology // Journal of Open Source Software. – 2022. – Vol. 7. – DOI: 10.21105/joss.04200.
36. Zoete V., Daina A., Bovigny C., Michielin O. SwissSimilarity: a web tool for low to ultra high throughput ligand-based virtual screening // Journal of Chemical Information and Modeling. – 2016. – Vol. 56. – P. 1399–1404. – DOI: 10.1021/acs.jcim.6b00174.